

SIGN SINGULARITY OF THE MAGNETIC HELICITY FROM IN SITU SOLAR WIND OBSERVATIONS

VINCENZO CARBONE¹ AND ROBERTO BRUNO²

Received 1996 October 28; accepted 1997 May 5

ABSTRACT

Some turbulent signed measures show a singularity related to extreme oscillations in sign, the scaling behavior of cancellations between positive and negative contributions being characterized by the cancellation exponent κ . Using in situ observations of magnetic fluctuations in the solar wind, we show that magnetic helicity is sign singular, a property that underlies the dominance of a single sign of polarization of fluctuations at small scales. We recover a statistical correlation between κ and the bulk solar wind speed when any correlation has been found between κ and the distance from the Sun. Even if the usual models of magnetic fluctuations based on random phases are able to reproduce (in a statistical sense) the gross features of helicity fluctuations, they cannot reproduce the behavior of sign singularity.

Subject headings: MHD — solar wind — turbulence

1. INTRODUCTION

1.1. The Cancellation Exponent

Some time ago, Ott et al. (1992) showed that signals $f(x)$ (defined on $x \in L$) that strongly oscillate from positive to negative values might be characterized by a sign singularity. This was achieved by introducing a signed measure (Halmos 1974) associated with $f(x)$,

$$\mu_r(L_i) = \int_{L_i(r)} f(x) dx \Big/ \left| \int_L f(x) dx \right|, \quad (1)$$

where $L_i(r) \subset L$ represents a hierarchy of disjoint subsets of size r , covering the whole set L , and by investigating the scaling properties of the expected value of $|\mu_r|$ at the scale r :

$$\chi(r) = \sum_{L_i(r)} |\mu_r(L_i)|.$$

(The sum is extended to all boxes of size r covering the set L .) In particular, Ott et al. (1992) conjectured that the process of oscillation at every scale might be described by a scaling law with exponent κ , which can be defined through the relation

$$\lim_{r \rightarrow 0} \frac{\log \chi(r)}{\log r} = -\kappa. \quad (2)$$

For a probability measure that is positive definite, $\chi(r) = 1$ and equation (2) yields the trivial value $\kappa = 0$. The scaling exponent vanishes also, if, below a certain cutoff r_s , the measure acquires a smooth density with a well-defined sign. In order to get a positive value for κ , $\chi(r)$ must increase without limit as $r \rightarrow 0$, which implies a singular behavior [$\chi(r)$ eventually saturates at scales r_s due to the presence of diffusive effects that smooth the measure]. In this case, the measure is said to be sign singular (Ott et al. 1992). Since the singular behavior occurs only if the cancellations between positive and negative contributions in μ_r are reduced (in the limit $r \rightarrow 0$), the exponent κ can be viewed as a quantitative characterization of the very rapid oscillations in the sign of

$f(x)$, and is called the *cancellation exponent*. From data analysis, the cancellation exponent is usually recovered by looking at the scaling law $\chi(r) \sim r^{-\kappa}$ in a range of values $r_s \leq r \leq r_0$ [if there is no saturation of $\chi(r)$, r_s is the minimum scale allowed in the data set].

Nontrivial examples of physical situations displaying the kind of singularity described above come from dynamo action (Ott et al. 1992; Du & Ott 1993a, 1993b; Lawrence, Ruzmaikin, & Cadavid 1993); fully developed turbulence (Ott et al. 1992; Bertozzi & Chhabra 1994; Vainshtein, Du, & Sreenivasan 1994a; Vainshtein et al. 1994b; Carbone 1995; Carbone & Bruno 1996), or simple random processes (Bertozzi & Chhabra 1994; Carbone et al. 1995). An effort to clarify the relations between κ and other scaling exponents characterizing fully developed turbulence—for example, the scaling exponents of the structure functions or the set of generalized dimensions D_q —has been made by Vainshtein et al. (1994b) for fluid flows and by Carbone & Bruno (1996) for MHD flows.

In particular, it has been shown that $0 \leq \kappa \leq 1$, even if some nontrivial examples where $\kappa > 1$ have been reported (Du & Ott 1993a). Apart from $\kappa = 0$, which indicates the absence of cancellations, critical values are $\kappa = 1$, which can be obtained in general for nondifferentiable fields (Vainshtein et al. 1994b), and $\kappa = \frac{1}{2}$, which is recovered in Brownian motion or in general stochastic processes (Bertozzi & Chhabra 1994; Vainshtein et al. 1994b). In general, given a stochastic process $f(x)$ with a Hölder exponent h , say $\langle |f(x+r) - f(x)| \rangle \sim r^h$ (where angular brackets mean averages), the cancellation exponent of its derivative is simply given by $\kappa = 1 - h$.

1.2. Magnetic Helicity

The helicity of the fluctuating magnetic field $\mathbf{B} = \nabla \times \mathbf{A}$, is defined as the volume-integrated quantity

$$H_m = \int \mathbf{A} \cdot \mathbf{B} d^3r$$

and represents a measure of linkage of flux tubes, or of the lack of mirror symmetry in MHD (Moffat 1978). In the absence of dissipation, H_m is a “rugged invariant” (Moffat 1978) and plays a key role in the turbulent dynamic of a magnetofluid (Ting, Matthaeus, & Montgomery 1986). Information about the magnetic helicity, when the available measurements are single-satellite observations, is contained

¹ Dipartimento di Fisica, Università della Calabria, 87030 Roges di Rende, Cosenza, Italy.

² Istituto di Fisica dello Spazio Interplanetario, C.P. 27, 00044 Frascati, Italy.

in the antisymmetrical terms of the spectral magnetic energy tensor (Matthaeus, Goldstein, & Smith 1982). In other words, from observations we get only a “reduced” magnetic helicity, defined through the trace of the Fourier transform $H_{ij}(k)$ of the symmetric part of the $\langle \mathbf{B} \cdot \mathbf{A} \rangle$ correlation

$$H_m^{(r)}(k_x) = \int dk_y dk_z \text{Tr} [H_{ij}(k)],$$

where x is the outward radial direction and z is the direction out of the ecliptic. It can immediately be seen that

$$H_m^{(r)}(k_x) = \frac{2 \text{Im} [S_{yz}^{(r)}(k_x)]}{k_x} \quad (3)$$

(Matthaeus et al. 1982), where

$$S_{yz}^{(r)}(k_x) = \frac{1}{2\pi} \int dx \exp(-ik_x x) R_{yz}(x, 0, 0)$$

is the Fourier transform of the correlation function

$$R_{yz}(x, 0, 0) = \langle B_y(\mathbf{r}) B_z(\mathbf{r} + x\mathbf{e}_x) \rangle.$$

It can be shown that in homogeneous turbulence

$$H_m = \int dk_x H_m^{(r)}(k_x)$$

(Matthaeus et al. 1982). It is also useful to define a dimensionless quantity, such as

$$\sigma(k) = \frac{k H_m^{(r)}(k)}{E_m^{(r)}(k)}, \quad (4)$$

where $E_m^{(r)}(k)$ is the reduced magnetic energy. This quantity, which is bounded by $|\sigma(k)| \leq 1$, represents the correlation between the two transverse components of the magnetic field \mathbf{B} when one of them is shifted by a factor of $\pi/2$ in phase. Then $\sigma(k)$ gives a measure of the polarization state of magnetic fluctuations: plane-polarized waves have $\sigma(k) = 0$, while right- or left-circularly polarized waves have, respectively, $\sigma(k) = \pm 1$.

Measurements in the solar wind show that magnetic turbulence at small scales is made by a superposition of fluctuations of (apparently) random polarization state (Matthaeus et al. 1982; Bruno & Dobrowolny 1986; Goldstein, Roberts, & Fitch 1991, 1994; Valdés-Galicia, Ataola, & Saulés 1993). That is, $\sigma(k)$ is a strongly oscillating function (see Fig. 1 and Goldstein et al. 1991, 1994). Furthermore, an interesting property, previously reported by Goldstein et al. (1991), is that, at small scales, a single sign of polarization dominates that is correlated with the direction of the magnetic sector polarity (Goldstein et al. 1994). These properties can be reproduced in a statistical sense by simple models of plane Alfvén waves with a random polarization (Barnes 1981; Goldstein et al. 1991).

In the following sections, we argue that a signed measure obtained from magnetic helicity is the natural way to describe the net polarization of magnetic fluctuations at a given scale. We show that the measure derived from magnetic helicity in the solar wind exhibits sign-singular behavior.

2. DATA ANALYSIS

The present analysis is based on $\Delta t = 81$ s averages of the magnetic vector $\mathbf{B}(t)$, recorded by *Helios 2* on its primary

mission in 1976. The spacecraft, while moving on the ecliptic, explored the inner heliosphere between 1 and 0.3 AU and within a latitudinal belt of $\pm 7.25^\circ$. This data set covers an interval of time that started on day 22 of 1976 and ended on day 114.

It is worthwhile to remark that one of the fundamental assumptions in analyzing solar wind fluctuations is the “frozen-in” approximation, which is the MHD analog of the Taylor hypothesis in fluid dynamics (see Tu & Marsch 1995). Under this assumption, the wavevector k_x is related to the frequency in the spacecraft frame $k_x = \omega/V_{sw}$, where V_{sw} is the bulk solar wind speed. Strictly speaking, this is true as long as we consider spatial scales smaller than the large-scale L of variation of the bulk magnetic field B_0 . On the other hand, the super-Alfvénic nature of the solar wind,

$$V_{sw} \gg \frac{B_0}{\sqrt{4\pi\rho}},$$

where ρ is the plasma mass density, implies that fluctuations remain almost unchanged while they are convected outward by velocity V_{sw} .

Since the in situ satellite observations give the one-dimensional magnetic field time series $\mathbf{B}(t)$, taking the Taylor hypothesis into account, magnetic helicity values as a function of frequency were computed by fast Fourier transform (FFT) of $B_y(t)$ and $B_z(t)$ components, thus obtaining

$$H_m^{(r)}(\omega) = \frac{2 \text{Im} [b_y^*(\omega) b_z(\omega)]}{\omega}, \quad (5)$$

where $b(\omega)$ represents the complex Fourier coefficients of \mathbf{B} at frequency ω . The normalized helicity is then given by

$$\sigma(\omega) = \frac{\omega H_m^{(r)}(\omega)}{|b_y(\omega)|^2 + |b_z(\omega)|^2}. \quad (6)$$

The frequency spectrum was based on a time interval of 2048 magnetic data samples of 81 s each, and, consequently, the frequency window spanned the range 6.03×10^{-6} – 6.17×10^{-3} Hz. This frequency range was divided into six frequency bands equally spaced in a logarithmic scale, and an average value of $\sigma(\omega)$ was evaluated and stored for each band. Successively, the time interval was shifted by one single 81 s average and the whole computation repeated. In this way we made $\sim 10^5$ estimates of $\sigma(t)$ [the Fourier anti-transform of $\sigma(\omega)$] for each of the six frequency bands. A running interval of 4200 values of $\sigma(t)$ was repeatedly shifted by one single 81 s estimate of $\sigma(t)$, and the value of the cancellation exponent was determined each time (see § 3). This technique provided $\sim 10^5$ estimates of κ for each frequency band.

After a preliminary analysis, only two frequency bands were chosen as fully representative of low- and high-frequency fluctuations, namely 6.6×10^{-5} – 1.9×10^{-4} Hz for the low-frequency (LF) band and 1.9×10^{-3} – 6.2×10^{-3} Hz for the high-frequency (HF) band. The whole process described above was repeated in order to construct a second data set in which the spectral components of $B_y(t)$ and $B_z(t)$ were artificially randomly phased. Results from both data sets will be analyzed and discussed in the next section. Occasionally, for some selected and short intervals, we repeated the analysis by using 6 s magnetic averages, and we were able to establish the fact that higher resolution data had no relevant effect on our results. Thus, due to the remarkable amount of data to be analyzed,

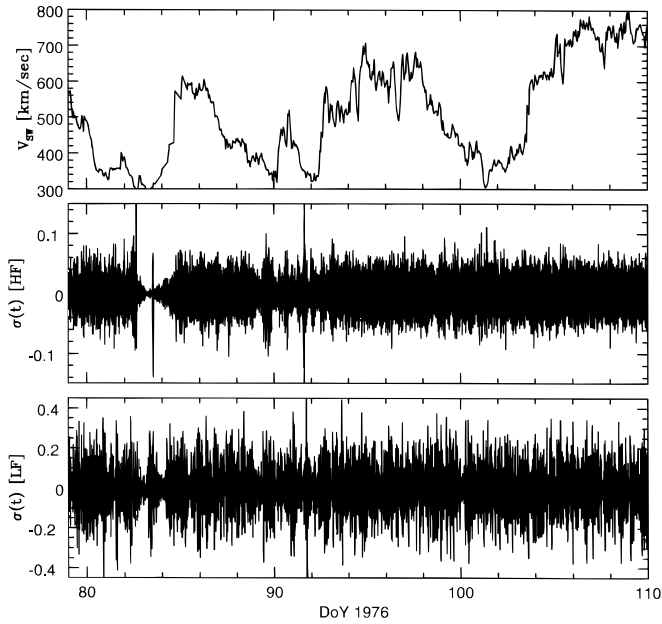


FIG. 1.—Time evolution of bulk solar wind velocity V_{sw} (upper panel) and normalized magnetic helicity $\sigma(t)$ in both high-frequency (middle panel) and low-frequency bands (lower panel). The selected time interval is from day 79 at 0.61 AU up to day 110 at 0.29 AU.

we decided to use the 81 s lower resolution data in order to reduce computer time.

3. SIGN-SINGULARITY OF MAGNETIC HELICITY

In Figure 1 we show the time evolution of $\sigma(t)$ for a given period of observation in both the HF and the LF band. The strong oscillatory character of this quantity is evident in both bands, thus suggesting the introduction of signed measures to investigate the net content of polarization at each

scale. However, looking at this figure, it is hard to recognize either any scaling behavior or any difference between the LF and HF bands.

As described in the previous section, we have selected a running interval of $T = 4200 \Delta t \approx 3.94$ days and calculated the instantaneous value of the function

$$g(t) = \frac{\sigma(t)}{\int_T \sigma(s) ds}.$$

The value we have chosen for T roughly corresponds to the average duration of a typical stream structure (Tu & Marsch 1995). Then, by using a partition of each domain T into boxes $T_i(\tau)$ of size $\Delta t \leq \tau \leq T$, we calculated

$$\chi(\tau) = \sum_{T_i(\tau)} \left| \int_{T_i(\tau)} g(t) dt \right|.$$

In Figure 2, we plotted $\log \chi(\tau)$ against $\log (\tau/T)$ for two typical periods of observation characterized by low and high speed, respectively. As can be seen, the gross features look different in the two frequency bands, while they are quite similar for slow and high-speed wind.

In the LF band, we see an increase of $\chi(\tau)$ up to a scale $\tau/T \approx 3.2 \times 10^{-3}$ (roughly corresponding to a scale $\tau \approx 0.3$ hr), beyond which the measure saturates. This behavior has been discussed extensively in the literature (see Bertozzi & Chhabra 1994, or reference 9 of Ott et al. 1992), where it is attributed to a small-scale cutoff (due to the small, diffusive length scale in Kolmogorov turbulence), which generates a smoothness in the density of the signed measure. In our case, the saturation is due to the fact that, by disregarding the high frequencies, we enhance the strong dominance of the large-scale magnetic field, which appears to be structured. As a consequence, the cancellations proceed until τ reaches the scale of variation of the measure, where further cancellations are stopped. On the other hand, the slope of

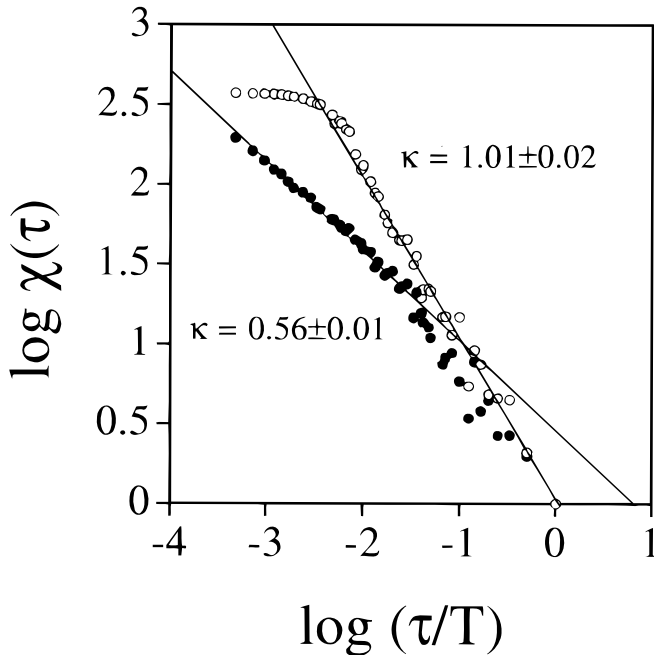


FIG. 2a

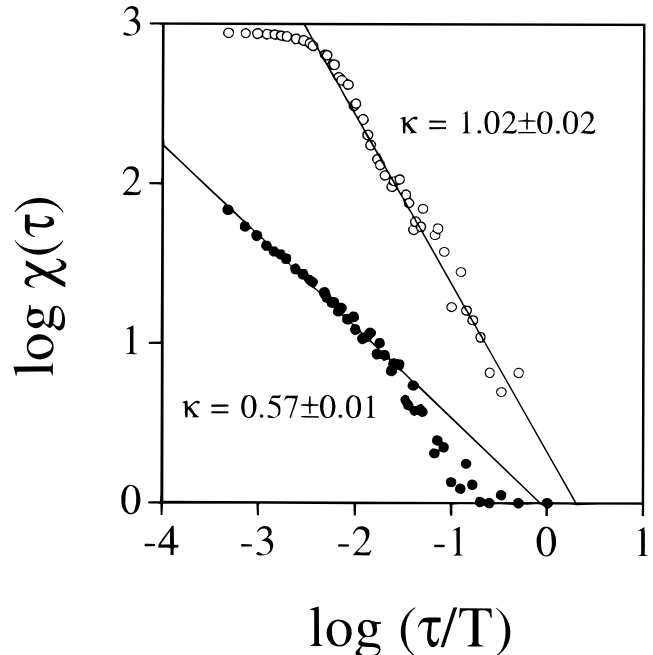


FIG. 2b

FIG. 2.— $\log \chi(\tau)$ vs. $\log (\tau/T)$ for two selected time intervals. The first interval corresponds to a high-speed stream located at 0.980 AU and starts on day 22 at 4:22:0 (a); the second interval corresponds to a low-speed stream at 0.972 AU on day 27 at 16:16:6 (b). Open circles refer to the low-frequency band, filled circles to the high-frequency band. The best fit of the data in a selected range (see text) is represented as a line.

the plot, for $\tau \leq 0.3$ hr, gives $\kappa \simeq 1$, thus indicating that the sign singularity is due to a nondifferentiable field (Vainshtein et al. 1994b). These properties are characteristic of a field with a strong dominance of structured large scales, as magnetic helicity appears from observations (Goldstein et al. 1991, 1994).

In the HF band, we observe a nice singular behavior: an increase of $\chi(\tau)$ up to the smallest available scale Δt . Beyond a crossover placed at approximately $\tau/T \simeq 3 \times 10^{-2}$ (roughly corresponding to a scale $\tau \simeq 3$ hr), we observe a well-defined scaling law covering more than two decades. This range of scales is usually called Alfvénic range (Tu & Marsch 1995), and MHD is considered to be the valid approximation for describing turbulence in this range (Tu & Marsch 1995). The behavior we found indicates that the cancellation between positive and negative polarizations is present at every scale in the whole Alfvénic range but *tends to decrease as $\tau \rightarrow 0$* . In other words, there exists a scaling property of magnetic fluctuations in the solar wind which underlies the previously observed dominance of a single polarization sign at high frequencies (Goldstein et al. 1991, 1994). The investigation of this property is the main goal of our paper.

We repeated the calculations for other periods but found no difference in the gross features just described. As noted in § 2, we repeated our calculations using 6 s resolution magnetic field averages. We did not find any departure from the results we presented here; the scaling law for the HF band, as reported in Figure 2, remains exactly the same: the increase of $\chi(\tau)$ continues up to the smallest scale with the same slope. This indicates that cancellations continue to reduce and that the eventual saturation drops well beyond a timescale of 6 s. In other words, magnetic helicity observed in the interplanetary medium shows a genuine sign singularity as far as high frequency is concerned.

4. COMPARISON WITH STOCHASTIC MODELS

In looking at these observations, we wonder whether stochastic models of magnetic fluctuations (Barnes 1981; Goldstein et al. 1991, 1994) can reproduce the singular behavior we observed in helicity fluctuations. To this end, we introduce a simple numerical procedure in the same spirit as the model introduced by Barnes (1981); that is, we make a randomization of the phases of the observed fields $\mathbf{B}(t)$. In other words, from $\mathbf{B}(t)$ we calculate the Fourier transform $b_j(\omega) = B_j(\omega) \exp [i\alpha_j(\omega)]$, then replace each $\alpha_j(\omega)$ by a random number uniformly distributed in the range $[0, 2\pi]$, and finally, we Fourier antitransform, thus obtaining a stochastic time series $\mathbf{B}_R(t)$. Our feeling is that singularities are mostly related to very localized and strong fluctuations in the real space, which are then characterized by phase correlations. These singularities can be observed, for example when looking at the usual multifractal behavior of the interplanetary magnetic field (Burlaga 1992; Burlaga & Ness 1996; Lawrence, Cadavid, & Ruzmaikin 1996). Our model simply destroys these correlations, leaving unchanged the net helicity content at each frequency, provided the power spectrum of the magnetic helicity is exactly that observed. Note that in the usual stochastic models (Barnes 1981; Goldstein et al. 1991), the spectrum of magnetic helicity is generally fixed a priori.

With the new fields $\mathbf{B}_R(t)$, we calculate a new normalized helicity $\sigma_R(t)$ and a new partition function $\chi_R(\tau)$, whose scaling against τ/T is shown in Figure 3. The difference between the plot and that shown in Figure 2 is evident. If phase correlations are destroyed, we observe the sign singularity due to a pure random field: a scaling law covering the whole range of τ with a cancellation exponent close to $\frac{1}{2}$, independent of the frequency domain (Bertozzi & Chhabra 1994; Vainshtein et al. 1994b; Carbone et al. 1995).

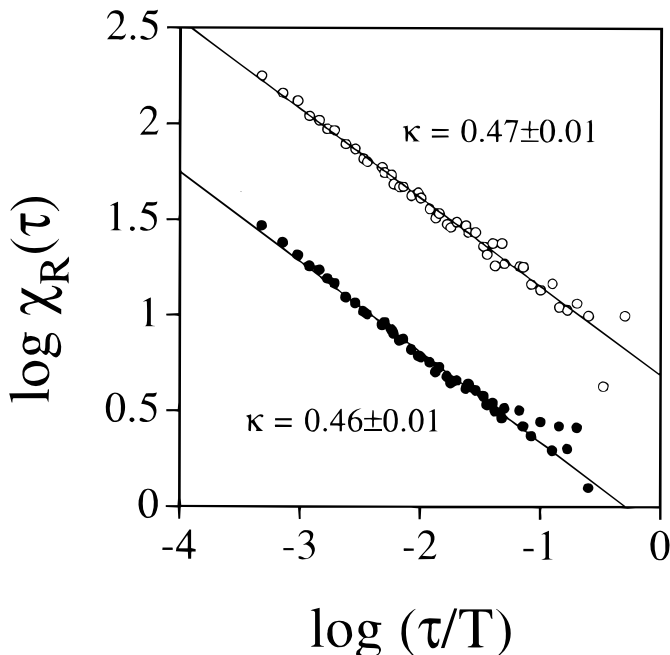


FIG. 3a

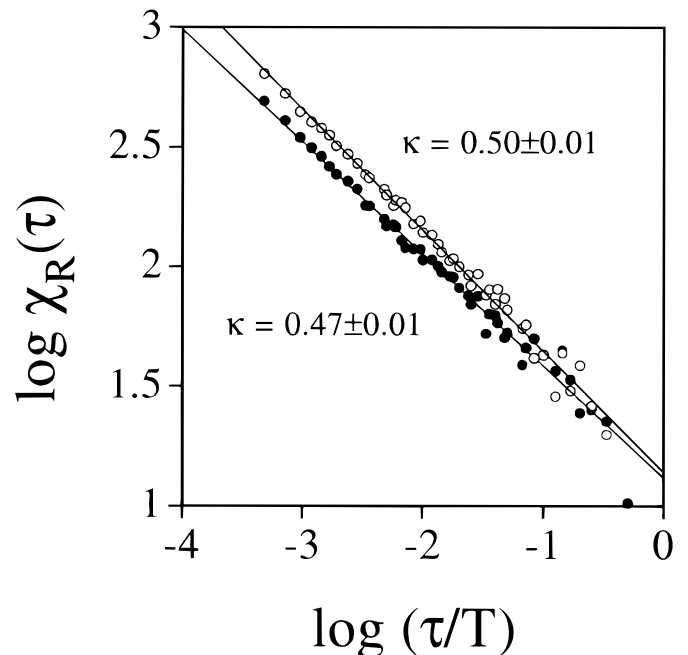


FIG. 3b

FIG. 3.— $\log \chi_R(\tau)$ vs. $\log (\tau/T)$ for the same data as in Fig. 2, but obtained from randomized time series. (a) refers to high-speed wind and (b) to low-speed wind.

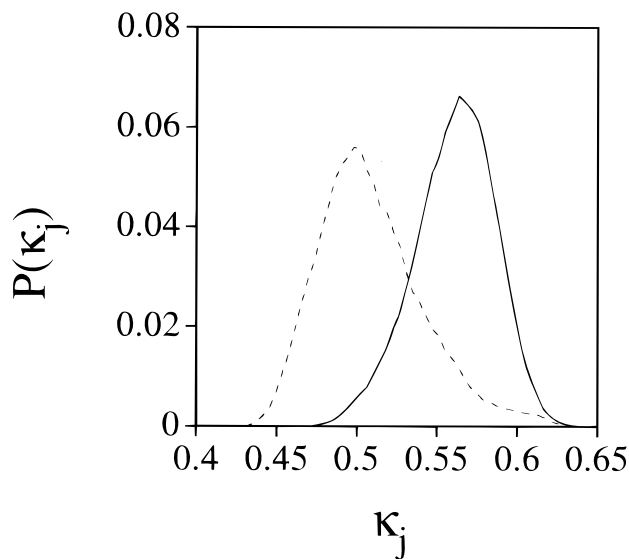


FIG. 4.—Probabilities $P(\kappa_j)$ against the bins κ_j of values of κ , obtained for the whole data set. Solid line refers to real data, dashed line to randomized data.

In the following, we will examine the HF band only. We have calculated values of the cancellation exponent for all the *Helios* data by linear fits in the Alfvénic range $\tau \leq 3$ hr, as described previously. Since the scaling law is well defined for all the data sets, the calculation of κ is very accurate, the error (estimated as the standard deviation for each fit) being within 5% of the value of κ . We have then divided the set of 10^5 values of κ so obtained into different bins, and we calculated the number $N(\kappa_j)$ of values of κ which fall within the j th bin. The results are summarized in Figure 4, where we

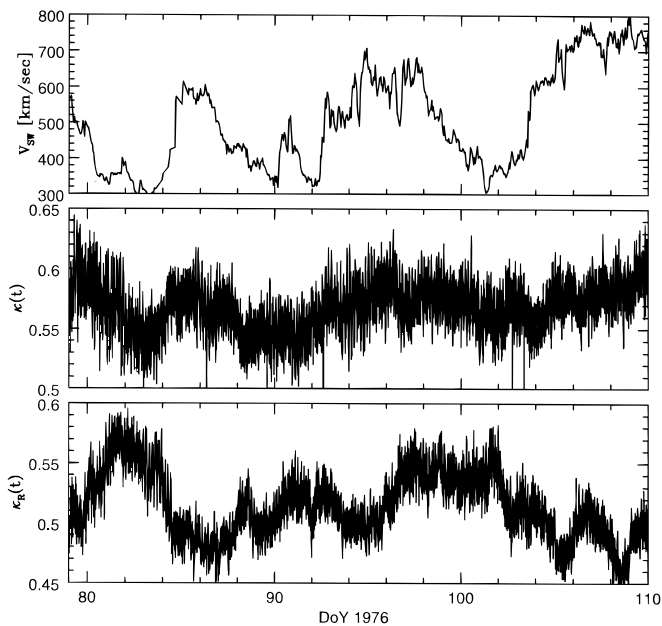


FIG. 5.—Time evolution of the bulk solar wind velocity V_{sw} (upper panel) and of the cancellation exponent κ obtained in the period from day 79 at 0.61 AU to day 110 at 0.29 AU. The middle panel refers to values of κ obtained from real data, the lower panel to values κ_R obtained from randomized data.

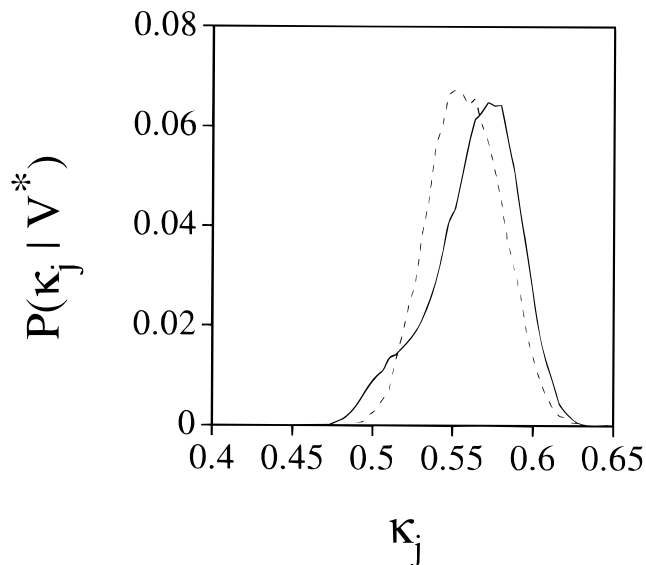


FIG. 6.—Conditional probabilities $P(\kappa_j | V^*)$ against the bins κ_j , calculated for the whole data set. Solid line refers to high-speed intervals ($V_{sw} \geq V^* = 500 \text{ km s}^{-1}$). Dashed line refers to low-speed intervals ($V_{sw} < V^* = 500 \text{ km s}^{-1}$).

plot the probability

$$P(\kappa_j) = \frac{N(\kappa_j)}{\sum_j N(\kappa_j)}$$

against κ_j for both real and randomized data. As can be seen, for both data sets there exists a distribution of values of κ_j , centered around the average value $\kappa \approx 0.576$ for real data and around $\kappa \approx 0.493$ for randomized data. The presence of a distribution of values is due to the fact that the cancellation exponent is related to other parameters, namely, the Hölder exponent h of the magnetic fluctuations, thus affecting the value of κ for the randomized data as well.

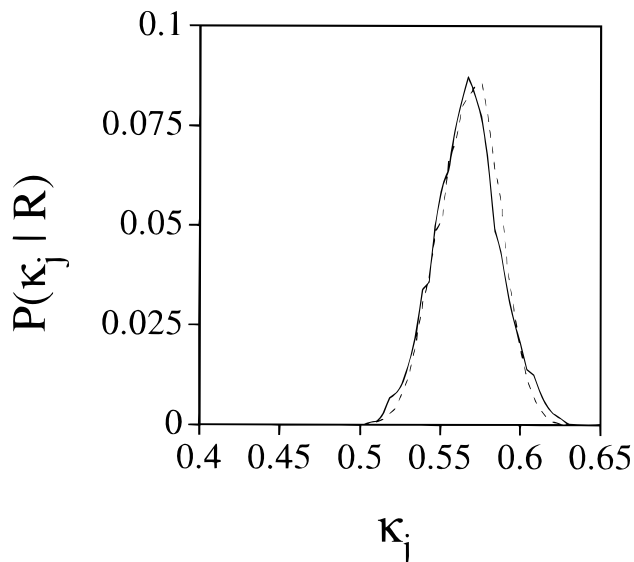


FIG. 7.—Conditional probabilities $P(\kappa_j | R)$ against the bins κ_j , calculated for the whole data set. Solid line refers to data from day 22 at 0.98 AU to day 30 at 0.96 AU, dashed line to data from day 89 at 0.49 AU to day 108 at 0.29 AU.

However, the reliable difference between the distribution obtained from real data and that obtained from randomized data is striking.

Since κ is related to the actual value of h , we expect it to depend on the physical properties of the periods we examined. To see whether this is the case, in Figure 5 we show the values of κ obtained for both $\sigma(t)$ and $\sigma_R(t)$, superimposed on the bulk speed V_{sw} of the solar wind, calculated for a certain period. As can be seen, there exists an evident correlation between κ (obtained with the observed magnetic helicity) and V_{sw} : roughly speaking, κ is greater when V_{sw} is high. This is not observed in the randomized time series (Fig. 5, lower panel). To see whether this is statistically meaningful, we calculate the probabilities $P(\kappa_j | V^*)$, conditioned on values of the bulk solar wind speed; that is, in building $N(\kappa_j)$, we take into account only values of κ corresponding to selected periods where V_{sw} is respectively higher or lower than a certain value V^* . In Figure 6 we report the results relative to $V^* = 500 \text{ km s}^{-1}$, a crossover value that roughly separates low-speed periods from high-speed periods. We detect two distinct peaks in the distributions, implying that the correlation between κ and V_{sw} does, in fact, exist. Moreover, in Figure 7 we report the values of the conditioned probabilities $P(\kappa_j | R)$, calculated by taking into account only selected periods at $R = 0.3 \text{ AU}$ (from day 98 to day 108) and at $R = 0.9 \text{ AU}$ (from day 22 to day 30). As can be seen, the distributions of the values of κ are roughly independent from the distance from the Sun.

5. SUMMARY AND DISCUSSION

This paper aims toward the investigation of the scaling behavior of magnetic helicity from in situ solar wind measurements. Since magnetic helicity is not positive definite, we must introduce a signed measure and investigate how much cancellation of opposite-sign measure takes place on fine scales. A quantitative characterization of this scaling process is given by the cancellation exponent. Our results can be summarized as follows:

1. Magnetic helicity in the solar wind is a sign-singular field. This means that there exists a scaling process underlying the reduction of cancellations between positive and negative helicities as the scale $\tau \rightarrow 0$. This phenomenon yields the dominance of a single polarization state of magnetic fluctuations at the smallest scales. The presence of even a small net content of helicity at these scales has been observed previously by Goldstein et al. (1991, 1994) (see also

Valdés-Galicia et al. 1993), who conjectured that plasma instabilities, like cyclotron damping, should be at work, acting as a selection mechanism for polarizations of different signs. As a rough estimate, the ion-cyclotron frequency in the solar wind turns out to be of the order of $\omega_i^{-1} \simeq 1 \text{ s}$. We showed that the process that generates the imbalance at the smallest scales is a scaling process, being due to a sign singularity. This means that the cancellations are self-similar on every scale involved in the process; that is, they are characterized by the scaling exponent κ rather than by an amplitude at a certain scale. Then, from a physical point of view, the selection mechanism acting on the polarization sign must act not only on the smallest scales but also on larger scales, as in the whole range $\tau \leq 3 \text{ hr}$. On these scales, usually called the “Alfvénic range” (Tu & Marsch 1995), MHD theory is reliable, so we expect that the selection mechanism should be an MHD mechanism. Since we found no saturation at the smallest available scale, and the scaling law is visible without any break, we can infer that the instability which generates the singular behavior must also be reliable in the MHD range.

2. The scaling exponent κ of the singularity seems to be correlated with the bulk speed of the solar wind. This is to say that, quite reasonably, the cancellations of right-hand and left-hand polarizations depend on the physical properties of the magnetic turbulence. They depend, actually, on the Hölder exponent h of magnetic fluctuations (Bertozzi & Chhabra 1994), for example on the slope of the power spectrum of magnetic helicity.

3. Even if the usual models of magnetic fluctuations, based on random phases (Barnes 1981), reproduce in a statistical sense the observed behavior of $\sigma(t)$ (Goldstein et al. 1991, 1994), they cannot capture the sign singularity and the correlations between κ and V_{sw} , which are based on strong phase correlations probably due to the multifractal properties of the interplanetary magnetic field (Burlaga 1992; Burlaga & Ness 1996; Lawrence et al. 1996).

We hope that our observations can stimulate the building of more refined models in which phase correlations are taken into account. A tentative effort in this direction is in progress.

We are grateful to F. Mariani and N. F. Ness for making the *Helios* magnetic data available to us and to the referee, James Chen, whose comments have improved the final version of the paper.

REFERENCES

- Barnes, A. 1981, *J. Geophys. Res.*, 86, 7498
 Bertozzi, A. L., & Chhabra, A. B. 1994, *Phys. Rev. E*, 49, 4716
 Bruno, R., & Dobrowolny, M. 1986, *Ann. Geophys.*, 4, A-17
 Burlaga, L. F. 1992, *J. Geophys. Res.*, 97, 4283
 Burlaga, L. F., & Ness, N. F. 1996, *J. Geophys. Res.*, 101, 13473
 Carbone, V. 1995, *Europhys. Lett.*, 29, 377
 Carbone, V., & Bruno, R. 1996, *Ann. Geophys.*, 14, 777
 Carbone, V., Lucchetta, D., Scaramuzza, N., & Versace, C. 1995, *Europhys. Lett.*, 32, 31
 Du, Y., & Ott, E. 1993a, *J. Fluid Mech.*, 27, 265
 ———, 1993b, *Physica D*, 67, 387
 Goldstein, M. L., Roberts, D. A., & Fitch, C. A. 1991, *Geophys. Res. Lett.*, 18, 1501
 ———, 1994, *J. Geophys. Res.*, 99, 11519
 Halmos, P. R. 1974, *Measure Theory* (New York: Springer)
 Lawrence, J. K., Cadavid, A. C., & Ruzmaikin, A. A. 1996, *ApJ*, 465, 425
 Lawrence, J. K., Ruzmaikin, A. A., & Cadavid, A. C. 1993, *ApJ*, 417, 805
 Matthaeus, W. H., Goldstein, M. L., & Smith, C. 1982, *Phys. Rev. Lett.*, 48, 1256
 Moffat, H. K. 1978, *Magnetic Field Generation in Electrically Conducting Fluids* (New York: Cambridge Univ. Press)
 Ott, E., Du, Y., Sreenivasan, K. R., Juneja, A., & Suri, A. K. 1992, *Phys. Rev. Lett.*, 69, 2654
 Ting, A. C., Matthaeus, W. H., & Montgomery, D. 1986, *Phys. Fluids*, 29, 3261
 Tu, C.-Y., & Marsch, E. 1995, *Space Sci. Rev.*, 73, 12
 Vainshtein, S. I., Du, Y., & Sreenivasan, K. R. 1994a, *Phys. Rev. E*, 49, R2521
 Vainshtein, S. I., Sreenivasan, K. R., Pierrehumbert, R. T., Kashyap, V., & Juneja, A. 1994b, *Phys. Rev. E*, 50, 1823
 Valdés-Galicia, J. F., Ataola, J. A., & Saulés, G. 1993, *J. Geophys. Res.*, 98, 21077